

Mathematical Modelling of Tumour Angiogenesis
and the Action of Angiostatin as a Protease Inhibitor*

Howard A. Levine
Department of Mathematics
Iowa State University
Ames
Iowa 50011
USA

Serdal Pamuk
Matematik Bölümü
Kocaeli Üniversitesi
Kocaeli, 41300
Turkey

Brian D. Sleeman
Department of Applied Mathematics
University of Leeds
Leeds
LS2 9JT, UK

Marit Nilsen-Hamilton
Department Biochemistry, Biophysics and Molecular Biology
Iowa State University
Ames
Iowa 50011
USA

Abstract

Tumour angiogenesis is the process whereby a capillary network is formed from a pre-existing vasculature in response to tumour secreted growth factors (TAF). The capillary network is largely composed of migrating endothelial cells which organize themselves into dendritic structures. In this paper we model angiogenesis via the theory of reinforced random walks, whereby the chemotactic response of the endothelial cells to TAF and their haptotactic response to the matrix macromolecule fibronectin is accomplished through transition probability rate functions. Tumour secreted growth and inhibitory factors are modeled on the basis of Michaelis-Menten kinetics. Particular attention is focussed on the action of anti-angiogenic agents (i. e. angiostatins). That is as a mechanism whereby angiostatin acts as a protease inhibitor. Numerical simulations yield results which are in good agreement with the experimental observations obtained by Folkman and his coworkers in their classical rabbit eye cornea experiments. The model offers a theoretical understanding of how some angiostatins work to inhibit tumour growth.

§0 Introduction

Angiogenesis is a morphogenic process whereby new blood vessels are induced to grow out of a pre-existing vasculature. It is fundamental to the formation of new blood vessels during embryonic development and contributes to the maintenance of tissue functionality in the

* Research supported by NSF-grant DMS-98-03992.

adult. An important example of the latter is placental growth. Angiogenesis is also an important feature of various pathological processes such as wound healing and cancer progression.

Capillaries, the main micro-vessels involved in tumour angiogenesis, are composed of three components (a) the basement membrane, which is a complex extra cellular matrix (ECM) encircling and supporting the cellular components, (b) the endothelial cells (EC) which form a mono-layer of flattened and extended cells lining the lumen and resting on the basement membrane and (c) pericytes which form a periendothelial cellular network embedded within the basement membrane.

The first event of tumour-induced angiogenesis is triggered by the secretion of a number of chemicals, collectively called Tumour Angiogenesis Factors (TAF) [Folkman, 85, 95, Folkman and Haudenschild, 80, Folkman and Klagsbrun 87] from a colony of cancerous cells of a solid tumour. These factors diffuse through the tissue creating a chemical gradient which eventually reaches neighbouring capillaries and other blood vessels. In response to TAF the EC in nearby capillaries appear to thicken and produce a proteolytic enzyme (protease) which in turn degrades the basement membrane. In further response to the TAF the normally smooth endothelial cell surface begins to develop pseudo podia which penetrate the weakened basement membrane. Capillary sprouts are formed by the accumulation of EC from the parent vessel. The sprouts grow in length, proliferate, form loops leading to micro-circulation of blood (i. e. anastomoses) and branch successively. The resulting capillary network continues to progress through the tissue ECM forming a micro vasculature, and eventually invades the tumour colony leading to rapid growth and metastasis. The means of progression through the tissue ECM is via chemotaxis and haptotaxis. Chemotaxis is the response of EC to chemical gradients set up by the TAF. A major component of the tissue ECM is fibronectin. It has been verified experimentally [Bowersox and Sorgente 82] that fibronectin stimulates directional migration of EC by establishing an adhesive gradient via haptotaxis.

Mathematical modelling of the complex processes involved in tumour angiogenesis has proceeded along two main fronts. Firstly there is the continuum approach based on differential equations developed from the principle of mass conservation and chemical flux considerations. This allows for a description of *macroscopic* events such as evolution of EC density and cell kinetic and migration characteristics as a result of chemotaxis and haptotaxis. The second avenue of investigation has been via discrete or cellular automata models in order to gain insight into the *microscopic* world of capillary network formation and to capture observations obtained from experiments *in vivo* and *in vitro*. For recent surveys of both these approaches we refer to [Sleeman, 96, Stokes and Lauffenburger 91, Chaplain-Anderson, 99].

In the case of continuum models we cite the recent work of Levine et al [Levine Sleeman, Nilson-Hamilton, 2000, 2001a,] in which a new approach to the initiation of angiogenesis is based on the idea of reinforced random walks, [Davis, 90, Othmer and Stevens 97, Levine-Sleeman 97] a key ingredient of the modelling to be pursued in this paper. At the microscopic level the behaviour of individual cells is fundamental to the understanding of capillary formation; particularly that of branching and anastomoses. cf [Stokes and Lauffenburger 91, Anderson-Chaplain 98 and the references given there]. Therefore, there is the challenging problem of understanding the "bridge" between micro and macro-cellular events. In the recent work of Sleeman and Wallis [Sleeman-Wallis 2000] it has been demonstrated that a possible key to establishing this connection is via the modelling of "transition rates" as exemplified in the work of Davis [Davis 90], Othmer-Stevens [Othmer-Stevens 97] and Levine et al [Levine et al 2000, 2001 a,b].

Angiostatin, a proteolytic fragment of the protein plasminogen is known to be a potent inhibitor of tumour angiogenesis. Indeed several angiogenesis inhibitor proteins exist as internal fragments of larger proteins (e.g. Prolactin) suggesting that normal angiogenesis inhibitors may be stored within larger proteins. When the body needs to stop normal angiogenesis, after wounding healing or ovulation for example, these natural inhibitors may be available for immediate use by breaking down the larger proteins [Hanahan and Folkman 96, Gorski et al 98, Falcone et al 98, Jendraschak Sage 96, O'Reilly et al 99]. It has also been discovered that these naturally occurring angiogenesis inhibitors are normally controlled by the tumour suppressor gene p.53 which has been implicated in various cancer types.

These important studies has lead to trials of anti-angiogenic drugs such as TNP-470 as a powerful new anti-cancer therapy. A primary goal of this paper is to model anti-angiogenic mechanisms and to attempt to understand how tumour angiogenesis may be inhibited.

The paper is organized as follows: In section 1 we describe the Boyden Chamber assay which is the basis for the modelling procedure. The chemistry of capillary sprout formation is considered in section 2 while in section 3 we discuss chemical models for the action of angiostatin. Using the laws of mass action and Michaelis-Menten kinetics (sections 3,4) the chemistry is reformulated as mathematical models of chemical transport both within the capillary as well as the ECM.

Endothelial cell transport, using the idea of reinforced random walks, is considered in sections 5 and 6. This completes the mathematical modelling.

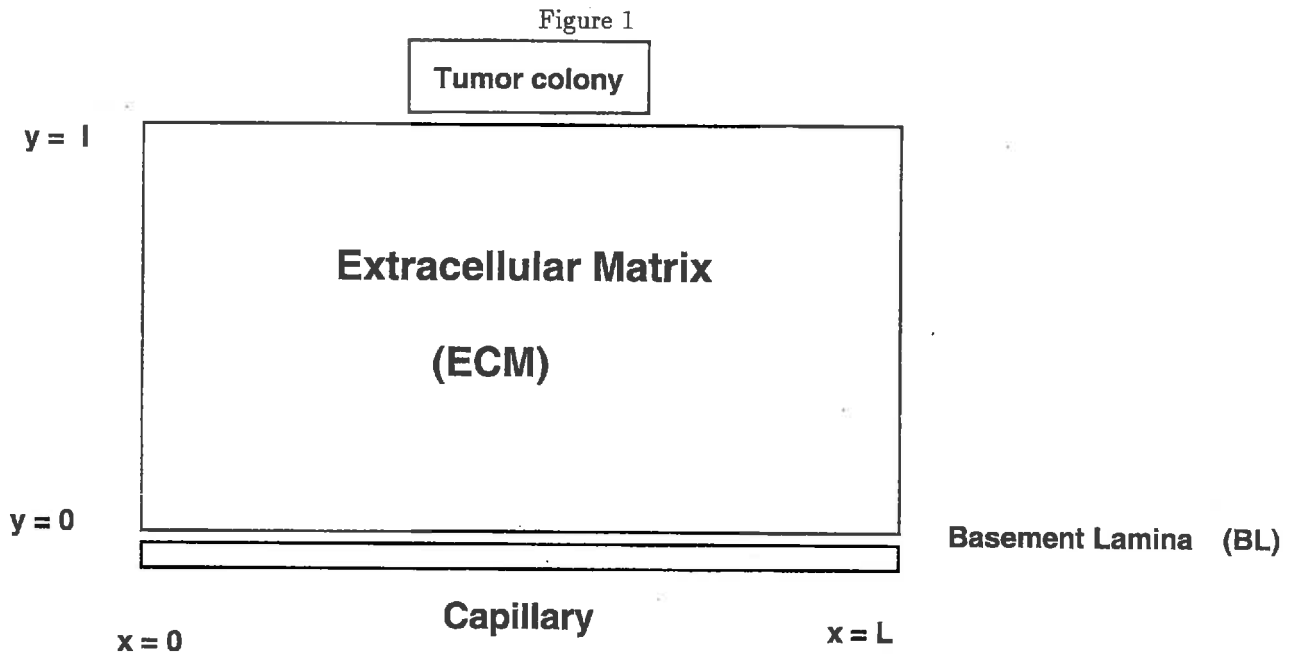
In §7 we discuss the results of a number of numerical experiments.

We conclude with a brief analysis of the results of the paper together with a discussion of possible therapeutic strategies which could be pursued in achieving angiogenic inhibition.

§1 Boyden Chamber Assay

Throughout this paper we base our modelling procedure on the simplified configuration shown in Figure 1. That is in the $x - y$ plane we envisage a capillary segment to be located along the x -axis on the interval $[0, L]$ with a tumour colony, or source of TAF, located ℓ units above the x -axis at $y = \ell$. The ECM is modelled as a porous medium. Alternatively, as in the Boyden Chamber Assay, the ECM may be a matragel bed in which case the ECM can be modelled as a viscoelastic medium. Such a configuration has been considered by several authors. See the review article of L. Tranqui and P. Tracqui [Tranqui-Tracqui 2000] and Holmes and Sleeman [Holmes-Sleeman 2000].

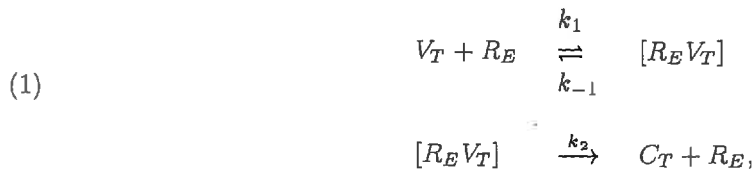
Time dependent quantities in the ECM will be represented by capital letters, eg $G(x, y, t)$ while quantities in the capillary will be denoted by lower case letters eg $g(x, t)$. It is important to note that in general $G(x, 0, t) \neq g(x, t)$.



§2 Biochemical Kinetics of Sprout Initiation

We begin by considering the initiation of elementary sprouts from the capillary wall. To better understand how tumour generated angiogenesis factors act on the EC we consider each EC has a certain number of receptors to which the angiogenic factor (ligand) binds. The bound molecules (intermediates) then stimulate the cell to produce a proteolytic enzyme and form new receptors.

Let V_T be the angiogenic factor (TAF) released by the tumour colony. Then we model the process as follows



where R_E denotes some receptor site on the EC surface membrane, $[R_E V_T]$ is the intermediate and C_T is a proteolytic enzyme produced as a consequence of this reaction. The proteolytic enzyme C_T now acts to degrade fibronectin (F) via the Michaelis-Menten catalytic reaction.



The Michealis-Menten condition is presumed to be in force here. This amounts to the statement that $[F C_T] = k_3[C_T][F]/k_4$.

This reaction reflects the fact that the enzyme degrades fibronectin, converting it into products F' by means of catalysis. It is to be emphasized that while the chemotactic agent V_T diffuses through the ECM from the tumour, it is converted almost immediately into receptor complexes upon arrival

at the capillary wall via the above reactions. Therefore we expect that the diffusion of these proteins along the capillary lumen is negligible in comparison to their conversion into receptor complex. [Levine et al 2001b]. However, the diffusion of these proteins cannot be neglected in the ECM. It is a major component of the transport mechanism for these proteins to and from the tumour.

§3 Models for the Action of Angiostatins

There are several possible ways in which angiostatic agents could inhibit angiogenesis. Here we discuss one possibility which has been verified in the experimental literature [Stack et al 1999]. That is we consider angiostatin A as a direct inhibitor of protease viz.



where C_A refers only to those molecules of proteolytic enzyme C_T that are available for the degradation of fibronectin. C_I denotes the proteolytic enzyme molecules which are inhibited by the angiostatin A from functioning as a catalyst for fibronectin degradation. In terms of concentrations $[C_T] = [C_A] + [C_I] + [C_A F]$. Assuming that (3) is in equilibrium, we have $[C_I] = \nu_e [A][C_A]$ where ν_e is the equilibrium constant for this step.

In general the reaction (3) is essentially complete. I.e., the equilibrium constant, ν_e , is quite large. However, the one example we have for this mechanism is to be found in the experimental work of Stack et al [Stack et al 99] where plasminogen activation is shown to be inhibited by angiostatin. (The tissue plasminogen activator (tPA) is produced in response to an angiogenic growth factor such as vascular endothelial cell growth factor ($VEGF$). Then tPA binds to plasminogen with the resultant product being plasmin (Pm). In the work of Stack et al [Stack et al 1999] it is proposed that angiostatin binds directly to the intermediate [$tPA - P_g$] complex to inhibit the production of active protease. The angiostatin here is a fragment of plasminogen with a molecular weight of about 38kDa. The literature value in [Stack et al 1999] given for ν_e^{-1} is of the order of $1\mu M$ which is not very large.

(We are currently preparing an article in which this entire process is modeled using the ideas elucidated below. Here we just employ the known equilibrium constant and the mechanism for angiostatin action.)

In the mechanism (3) the critical equation for the concentration of active enzyme is

$$(4) \quad [C_A] = \frac{[C_T]}{1 + \nu_e [A] + [F]/K_m^2}$$

where $K_m^2 = k_4/k_3$.

§4 Chemical Transport Equations in the Capillary

From the system of chemical reaction rate equations described in sections 2 and 3 we construct a mathematical model governing chemical transport in the capillary using the laws of mass-action and a careful use of Michaelis-Menten kinetics. We do not detail the derivations here but refer the reader to [Levine et al 2000, 2001a,b] for a full account of the development.

Introduce the notation

variable	In the capillary	In the ECM.
growth factor, V	$v(x, t)$	$V(x, y, t)$
proteolytic enzyme, C	$c(x, t)$	$C(x, y, t)$
active proteolytic enzyme, C_A	$c_a(x, t)$	$C_a(x, y, t)$
inhibited proteolytic enzyme, C_I	$c_i(x, t)$	$C_i(x, y, t)$
total available active enzyme, \tilde{C}_A	$\tilde{c}_a(x, t)$	$\tilde{C}_a(x, y, t)$
angiostatin, A	$a(x, t)$	$A(x, y, t)$
protease inhibitor, I	$i_a(x, t)$	$I_a(x, y, t)$
fibronectin, F	$f(x, t)$	$F(x, y, t)$
endothelial cell density	$\eta(x, t)$	$N(x, y, t)$

The chemical transport equations are given by

$$\begin{aligned}
 \frac{\partial v}{\partial t} &= -\frac{\lambda_1 v}{1 + \nu_1 v} \frac{\eta}{\eta_0} + v_r(x, t), \\
 \frac{\partial c}{\partial t} &= \frac{\lambda_1 v}{1 + \nu_1 v} \frac{\eta}{\eta_0} - \mu c, \\
 \frac{\partial f}{\partial t} &= \frac{4}{T_f} \left(1 - \frac{f}{f_0}\right) f \frac{\eta}{\eta_0} - \frac{\lambda_2 \tilde{c}_a f}{1 + \nu_2 f}, \\
 \frac{\partial a}{\partial t} &= a_r(x, t) - \frac{1}{T_{rel}} a(x, t), \\
 c_a &= \frac{c}{1 + \nu_e a + \nu_2 f} \\
 \tilde{c}_a &= c - c_i.
 \end{aligned}
 \tag{5}$$

This system models chemical transport when angiostatin is considered to be a direct inhibitor of protease as governed by (3). Here T_{rel} is the relaxation time for angiostatin decay.

In the system (5), ν_e is the equilibrium constant for (3) while $\lambda_1 = k_1 \delta_e \eta_0$, $\lambda_2 = k_3$, $\nu_1 = k_1 / (k_{-1} + k_2)$ and $\nu_2 = k_3 / k_4$. δ_e is the average number of receptors on an endothelial cell which bind to protease and η_0 is the EC density in a normal capillary. In addition the forcing term $v_r(x, t)$ allows for the rate at which TAF is produced by the tumour colony. Natural decay of enzyme c is modelled by $-\mu c$. It is known that EC produce fibronectin and this is accounted for by the introduction of the logistic growth term in (5) where f_0 is the maximum value of f .

For therapeutic purposes any angiostatic agent must be supplied at a rate $a_r(x, t)$ sufficient to "neutralize" the proteolytic enzyme until the tumour has been rendered inactive. A reasonable model for a_r might be a constant function, representing a constant rate of supply of anti-angiogenic drug.

§5 Chemical Transport Equations in the ECM

Within the ECM much the same chemistry applies as in the capillary. However there are significant modifications necessary.

First of all we assume that the background fibronectin production is in considerable excess of that produced by the endothelial cells, so that the logistic growth term in the analogous fibronectin dynamics (5) is independent of $N(x, y, t)$. Secondly we assume that in so far as growth factor and angiostatin are concerned, the ECM is a porous medium through which these chemicals diffuse.

Furthermore we do not assume that the diffusivities for these species, namely D_V, D_A are constant. Thirdly, we allow for inhomogeneous diffusion of growth factor and for angiostatin. That is we assume that molecules of either type visualize the ECM as a porous medium but with variable diffusivities D_V, D_A . Furthermore we assume that the porosity index 'm' is the same for both species. This is based on the fact that these two proteins are about the same size. This is not the only way in which the ECM can be modelled. For instance it may be considered to be a visco-elastic medium as considered in [Tranqui and Traqui 2000, Holmes and Sleeman 2000].

It is known that proteases must be bound to cell surfaces in order to effect cell migrations in the ECM [Alberts et al, 1994]. Hence no corresponding diffusion terms need to be included in the rate law for the proteolytic enzyme.

Finally we need to include the diffusivity of fibronectin within the ECM. Generally fibronectin diffuses slowly. However, it is reasonable to assume that its diffusion is curvature dependent. In our two dimensional configuration we model this via mean curvature.¹

From the above discussion, and keeping in mind the notational convention described in §1, the kinetics within the ECM are taken to be

$$\begin{aligned}
 \frac{\partial V}{\partial t} &= \nabla \cdot [D_V(x, y) \nabla V^m] - \frac{\lambda_1 V}{1 + \nu_1 V} \frac{N}{\eta_0} + V_r(x, y, t), \\
 \frac{\partial C}{\partial t} &= \frac{\lambda_1 V}{1 + \nu_1 V} \frac{N}{\eta_0} - \mu c, \\
 \frac{\partial F}{\partial t} &= D_F k(x, y) |\nabla F| + \frac{4}{T_F} \left(1 - \frac{F}{F_0}\right) F - \frac{\lambda_2 \tilde{C}_A F}{1 + \nu_2 F}, \\
 \frac{\partial A}{\partial t} &= \nabla \cdot [D_A(x, y) \nabla A^m] + a_r(x, t)(1 - F/F_0), \\
 C_A &= \frac{C}{1 + \nu_e A + \nu_2 F}, \\
 C_I &= \nu_e A C_A, \\
 \tilde{C}_A &= C - C_I.
 \end{aligned}
 \tag{6}$$

If $k < 0$, the growth rate for fibronectin (F_t) is diminished whereas if $k > 0$ the growth rate is increased.

In the first equation of (6) we have included a source term $V_r(x, y, t)$ to account for the situation in which growth factor is generated within the ECM. Furthermore we have included the source term $a_r(x, t)(1 - F/F_0)$ in the fourth equation of (6). This term allows us to introduce angiostatin in every region of the capillary network for which fibronectin density is below the background value F_0 in the ECM, at a rate which is proportional to the fibronectin deficit in the ECM.

¹If $z = \phi(x, y)$ then the curvature, for fixed z , of the level line is given by $k = \nabla \cdot \left(\frac{\nabla \phi}{|\nabla \phi|} \right)$. The inclusion of this term in the fibronectin equation is motivated by an idea taken from the theory of dendritic crystal growth. There, growth of dendrites occurs only at the tip where the local ratio of surface area to volume is greatest.

§6 Cell Transport in the Capillary and ECM

To model the transport of EC both within the capillary in response to the angiogenic growth factor and in the ECM we use, as in [Levine et al 2000, 2001 a,b] a continuum form of the idea of reinforced random walks developed by Othmer and Stevens [Othmer-Stevens 1997, Levine-Sleeman 1997]. That is, if η denotes the EC in the capillary wall then

$$(7) \quad \frac{\partial \eta}{\partial t} = D_\eta \frac{\partial^2 \eta}{\partial x^2} - D_\eta \frac{\partial}{\partial x} \left(\frac{\eta}{\tau} \frac{\partial \tau}{\partial x} \right).$$

In this equation τ is called the transition probability function and is modelled to reflect the fact that the EC respond both chemotactically and haptotactically respectively to gradients in proteolytic enzyme c and fibronectin f .

The interpretation of (7) is that the rate of change of EC is balanced by random diffusion and chemical sensitivity to c and f . The modelling of τ is a challenging problem. However from biological considerations [Levine et al 2000, 2001a,b] we take in our simulations

$$(8) \quad \tau(c_a, f) = \left(\frac{c_a + \alpha_1}{c_a + \alpha_2} \right)^{\gamma_1} \left(\frac{f + \beta_1}{f + \beta_2} \right)^{\gamma_2}$$

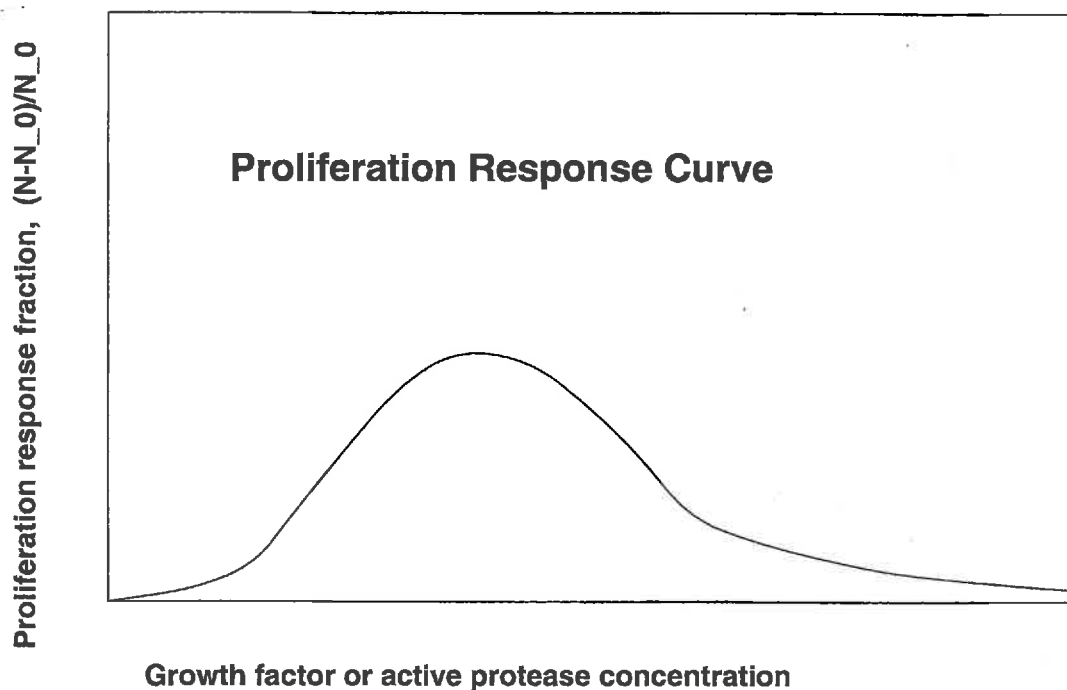
where $\alpha_i, \beta_i, i = 1, 2$ are empirical constants with $0 < \alpha_1 \ll 1 < \alpha_2, \beta_1 > 1 \gg \beta_2 > 0$. These choices of parameter ranges reflect the fact that EC aggregate towards high concentrations of c_a and to regions where f is most degraded. For full justification of the modelling of τ we refer to [Levine et al 2000, 2001 a,b].

To model the transport of EC within the ECM we need to take account of both the proliferation and apoptosis or death of cells. Specifically we write

$$(9) \quad \frac{\partial N}{\partial t} = D_N \Delta N - D_N \nabla \cdot (N \nabla T(C_A, F)) + Q(k) \left\{ N \left[\theta(N_s - N) + G(C_A) \frac{\partial C_A}{\partial t} \right] H(C_A - C_{A,0}) - \mu N \right\}.$$

In this equation the first two terms on the right hand side are the two dimensional analogs of the corresponding terms on the right of (9). The third term incorporates several important issues. First we have included a "logistic" proliferation rate of EC and a linear "death rate". It is known that proliferation of EC occurs only near the tip of growing capillaries and to account for this we have included a factor $Q(k)$ which is small when tip curvature k is small and large when the tip curvature is large. Furthermore it is also known that cell proliferation responds to active protease C_A in a biphasic manner and this has been modelled in (9) by the inclusion of the function $G(C_A)$ shown in Figure 2

Figure 2



Finally proliferation only occurs if the active protease C_A is above a certain threshold $C_{A,0}$. This is modelled in (9) by the inclusion of the "Switch" $H(C_A - C_{A,0})$ where H is the Heaviside Step function defined by

$$H(x) = \begin{cases} 1, & \text{if } x \geq 0, \\ 0, & \text{if } x < 0. \end{cases}$$

To complete this rather extensive mathematical model based on the chemical transport equations of sections 4 and 5 together with the EC equations of section 6 we must close the system with appropriate boundary and initial conditions. This is detailed in [Levine et al 2001b] and will be referred to appropriately in the numerical experiments discussed in the following section.

§7 Numerical Experiments

To begin with we adopt the phrase "onset of angiogenesis" to mean that a capillary sprout has been initiated from the pre-existing vasculature. By "onset of vascularization" we mean that a newly formed capillary has just reached the tumour colony.

In vivo one expects that tumour stimulated growth rate of new capillaries will depend on several variables. These would include chemical properties of growth factors and the proteases themselves

as well as the protein structure of the ECM. The model we have developed above reflects this dependency.

To connect the EC transport equations with the capillary wall and the ECM we assume that the EC in the capillary wall move into the ECM when the fibronectin density f in the capillary wall falls below a certain threshold level f_1 . That is we take

$$(10) \quad N(x, 0, t) = \psi_1 H(f_1 - f) \eta(x, t)$$

where $0 < \psi_1 \leq 1$ is interpreted as a measure of the fraction of EC lining the lumen that are able to penetrate the ECM.

We next assume that the tumour colony is supplying a prescribed flux of VEGF. In our experiments this flux is given by

$$(11) \quad V_t(x, t) = v_0 \frac{\sigma}{L} \left[1 - \cos\left(\frac{2\pi x}{L}\right) \right]^{m_0}$$

where σ is a fixed constant normalized so that the mean flux is v_0 . By lowering the threshold value of f_1 or by decreasing the dosage rate v_0 will have the effect of slowing the rate of onset of angiogenesis. Also by changing the percentage of EC's ψ_1 will effect capillary tip growth rate.

The coefficient $Q(k)$ in (9) is a curvature sensitivity factor and is taken to be

$$(12) \quad Q(k) = \frac{k}{\sqrt{1 + \varepsilon^2 k^2}}.$$

This choice is made not only because we want the curvature sensitivity to be dimensionless but also because we need to control the sensitivity to proliferation. Note maximum sensitivity is $Q_{max} = -1/\varepsilon$.

Finding good estimates for the constants used in the model is not an easy task. Fortunately with the help of Mr John E. Hinrichsen we were able to locate some constants and obtain order estimates for some others. The entries used in Table 4 of the appendix include those found as well as others used in our computations. In [Levine et al 2001b] the reader may find extensive references for the entries in Table 4.

In the first numerical experiment we implanted a "tumour" 25 microns from a pre-existing capillary. In Figure 3 we see the advance of EC across the ECM while in Figure 4 we observe the EC aggregate along the capillary wall. Notice the peak of EC density near the tip in Figure 3 and the bimodal distribution of EC density in Figure 4. In Figures 5 the degradation of fibronectin with time forming a channel through the ECM is seen. In Figure 6, one sees the degradation of the capillary wall.

In Table 1 we give the travel times to various points in the ECM after tumour implantation. The tip speeds in the third column are quite close to the tip speeds observed in Folkman, et al. The extrapolated times of one and two millimeter implant distances are also consistent with the travel times they observed. Furthermore, they observed that the tip speed increases with tip approach to the tumor. This is also the case for our simulated capillary tips.

TABLE 1. Travel times and tip speeds

Distance from mother capillary to tip of daughter ($\ell = 25\mu\text{mm}$)	Time in hours	Mean velocity (mm/day)	Extrapolated time in days for $\ell = 1\text{mm}$	Extrapolated time in days for $\ell = 2\text{mm}$
0.00	3.49		5.817	11.633
2.50	3.74	0.242	6.817	13.633
5.00	3.88	0.436	7.317	14.633
7.50	3.99	0.545	7.650	15.300
10.00	4.09	0.580	7.900	15.800
12.50	4.18	0.703	8.100	16.200
15.00	4.25	0.831	8.267	16.533
17.50	4.32	0.914	8.410	16.819
20.00	4.38	1.015	8.535	17.069
22.50	4.43	1.015	8.646	17.291

$$(\epsilon = 1.125, f_1 = 0.60, v_0 = 4.0\mu\text{Mmmh}^{-1}, L = 50\mu\text{mm})$$

Next we introduce angiostatin at the rate

$$(13) \quad a_r(x, t) = A_r H(t - T_{iv}).$$

Here A_r is the rate at which angiostatin is being supplied and T_{iv} is elapsed time since the tumour began to leak growth factor into the ECM. In our computations $T_{iv} = 4.1$ hours. We chose this time because for our choice of ν_e , the reaction (3) is not complete. This means that one either has to swamp the mother capillary with very high concentrations of inhibitor to bind the active protease in order to prevent tumor vascularization or else introduce the inhibitor relatively early in the growth of the daughter capillary. For purposes of illustration, we have opted for the latter.

Figure 7 shows the time course of EC propagation in the ECM before and after inhibitor introduction. Figure 8 gives the corresponding time courses for fibronectin in the ECM. Notice that there has been a marked drop in EC density although the closing of the fibronectin channel is somewhat more muted. However the closing of the capillary at the point where it begins to enter the ECM from the mother capillary can clearly be seen in Figure 8d. In Figure 9 we plot time courses within the mother capillary, of EC, fibronectin, protease and active protease in the presence of angiostatin. The dashed lines correspond to a time of 5.1 hours while the solid lines correspond to the time of 4.1 hours after the experiment has begun. Notice that the concentration of protease has fallen by about fifty percent while there is almost no active protease in the mother capillary. The opening (Figure 9b) in the fibronectin is also closing.

In Figures 10, 11, we see the effect of the introduction of angiostatin on the time courses of VEGF, inactive protease and active protease.

We next turn to an analysis of the dependency of endothelial cell movement across the ECM to capillary tip curvature k based on the curvature sensitivity factor, ϵ . To begin with we denote by T_α for $0 \leq \alpha \leq 1$ the time, in hours, from the onset of "tumour" implantation to the time the capillary tip has moved a fraction α of the distance ℓ from the capillary to the tumour colony. That is T_α is the time taken for some EC's to have moved a distance $\alpha\ell$ from the capillary located along the x-axis. The sensitivity of the travel times to the capillary tip sensitivity parameter ϵ is recorded in Table 2.

Notice that as ϵ increases, cell travel time across the ECM slows down. This is to be expected since curvature sensitivity decreases with increasing ϵ . Furthermore this will effect the rate of enzyme

degradation of fibronectin due to the fact that the rate of growth of protease is proportional to EC concentration. Consequently if protease concentration does not increase, the rate of fibronectin degradation will decrease. For example when $\epsilon = 0.5$, $\bar{V} = 0.24$ mm/day.

TABLE 2. Variable ϵ , curvature sensitivity.

$\epsilon \rightarrow$	0.900	1.00	1.10	1.20	1.30	1.40	1.50	1.60
T_0	1.18h	1.18h	1.18h	1.18h	1.18h	1.18h	1.18h	1.18h
$T_{\frac{1}{4}}$	1.247h	1.254h	1.28h	1.29h	1.31h	1.34h	1.38h	1.40h
$T_{\frac{1}{2}}$	1.28h	1.31h	1.36h	1.40h	1.44h	1.48h	1.52h	1.57h
$T_{\frac{3}{4}}$	1.29h	1.32h	1.38h	1.45h	1.51h	1.59h	1.66h	1.78h
T_1	1.31h	1.34h	1.41h	1.51h	1.61h	1.71h	1.82h	1.92h
\bar{v}	3.13 mm/d	2.55 mm/d	1.77 mm/d	1.16 mm/d	0.95 mm/d	0.77 mm/d	0.64 mm/d	0.55 mm/d

Mean tip speed is computed as $\bar{v} = 0.017/(T_1 - T_0)$ in millimeters per day.

($v_0 = 3.0 \mu M m m h^{-1}$, $f_1 = 0.40$, $\ell = 17 \mu m m$).

TABLE 3. Tumour/capillary distance sensitivity (variable ℓ).

$\ell \rightarrow$	17.0 μm	34.0 μm	51.0 μm	68.0 μm
mesh size \rightarrow	30 \times 20	30 \times 40	30 \times 60	60 \times 80
T_0	1.18h	2.26h	3.67h	5.37h
$T_{\frac{1}{4}}$	1.25h	2.43h	3.94h	5.80h
$T_{\frac{1}{2}}$	1.31h	2.53h	4.10h	5.98h
$T_{\frac{3}{4}}$	1.32h	2.57h	4.14h	6.05h
T_1	1.34h	2.59h	4.18h	6.13h
Mean tip speed	2.55 mm/day	2.47 mm/day	2.40 mm/day	2.15 mm/day

$v_0 = 3.0 \mu M m m h^{-1}$, $f_1 = 0.40$, $\epsilon = 1.0$

To investigate how the travel time across the "ECM" to the capillary and back to the tumour depends on the distance from the tumour to the ECM, the number ℓ , the sensitivity is fixed ($\epsilon = 1.0$) and ℓ is varied.

The results are shown in Table 3.

The table clearly shows that as the distance to the tumour increases the travel time, as expected, increases but the mean tip speed decreases.

§8 Conclusions and Discussion

In this paper a mathematical model of tumour angiogenesis has been described on the basis of the chemical kinetics governing the chemistry of angiogenic factors, protease activity as well as of fibronectin degradation and angiostatin interference in protease activity. The motion of endothelial cells both within the ECM and in the capillary wall is governed by a continuum limit of a reinforced random walk process.

Of particular importance is the angiostatic agent considered here as a direct inhibitor of protease as indicated in the experimental literature.

Using known literature values to the maximum extent possible, our numerical simulations give results that are in reasonable qualitative and quantitative agreement with the results of the rabbit eye cornea experiments of Folkman et al. In particular travel times of EC across the ECM towards the tumour are of the same order of magnitude as found in *in vitro* studies. The diameter of the

growing (numerical) capillary is of the order of 6–10 microns. It is also shown that capillary growth is sensitively dependent on tip curvature and hence on cell proliferation. The role of angiostatin as a direct protease inhibitor is included and shows that if angiostatin is administered soon after the onset of angiogenesis then growth of capillaries is greatly reduced and fibronectin degradation severely restricted.

Appendix

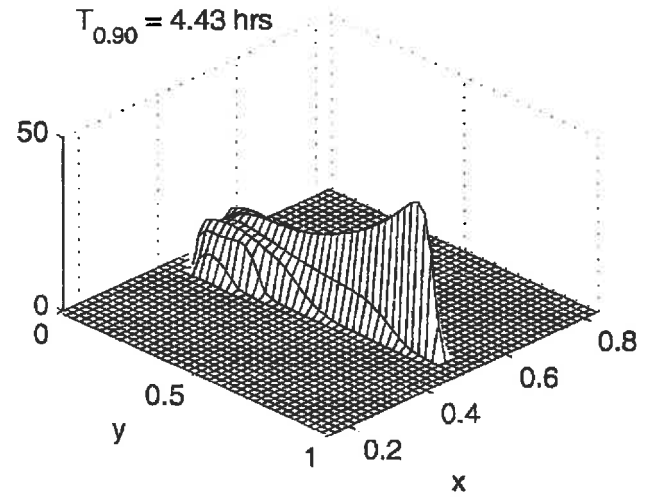
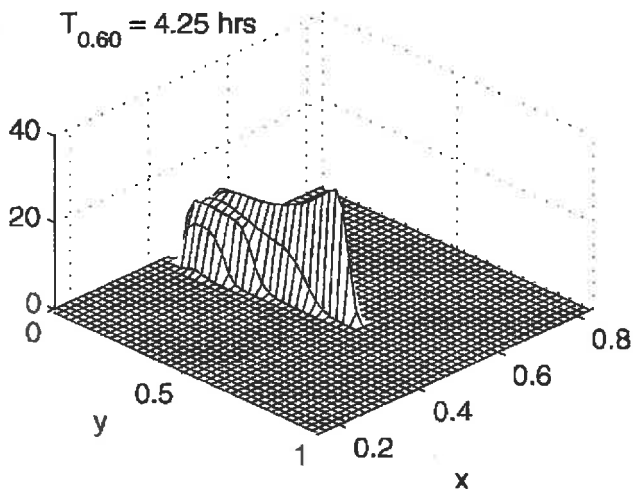
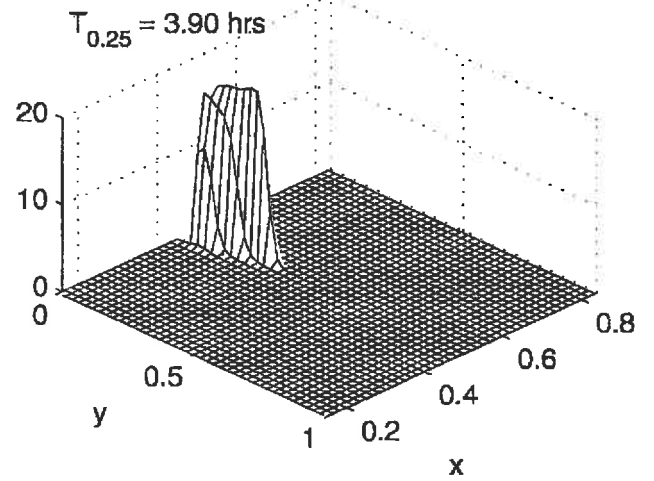
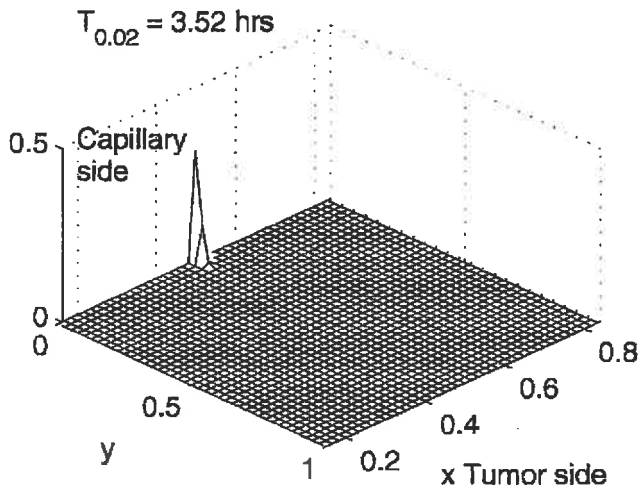
TABLE 4. Physiological and kinetic constants

(5)	$\lambda_1 = 73.0\mu M^{-1}h^{-1}$	$\nu_1 = 0.007\mu M^{-1}$	$\mu = 0.0$	
	$\lambda_2 = 146.0\mu M^{-1}h^{-1}$	$\nu_2 = 0.014\mu M^{-1}$	$\nu_e = 1.0\mu M^{-1}$	
(6)	$D_v = 3.6 \times 10^{-3}mm^2h^{-1}$	$\lambda_1 = 73.0\mu M^{-1}h^{-1}$	$\nu_1 = 0.007\mu M^{-1}$	$\mu = 0.0$
	$v_r(x, y, t) = 0.0\mu Mh^{-1}$	$\nu_e = 1.0\mu M^{-1}$		
(5)	$T_f = T_F = 18.0h = 4\beta^{-1}$	$\lambda_2 = 19.0\mu M^{-1}h^{-1}$	$\nu_2 = 1.28\mu M^{-1}$	$f_0 = F_0$
(5.1)	$D_F = 3.6 \times 10^{-8}mm^2h^{-1}$	$F_0 = 1.0 \times 10^{-3}\mu M$	$\lambda_2 = 19.0\mu M^{-1}h^{-1}$	$nu_2 = 1.28\mu M^{-1}$
(7)	$D_n = 3.6 \times 10^{-6}mm^2h^{-1}$	$\alpha^1 = 0.1\mu M$	$\alpha_2 = 1.0\mu M$	$\gamma_1 = 4.0$
		$\beta_1 = 1.0\mu M$	$\beta_2 = 0.1\mu M$	$\gamma_2 = 4.0$
(9), (12)	$D_N = 3.6 \times 10^{-6}mm^2h^{-1}$	$\alpha_1 = 0.1\mu M$	$\alpha_2 = 1.0\mu M$	$\gamma_1 = 2.0$
	$\epsilon = 1.40$	$\beta_1 = 1.0\mu M$	$\beta_2 = 0.5\mu M$	$\gamma_2 = 1.5$
	$\gamma = 1.1 \times 10^{-9}\mu M^{-2}$	$m_1 = 2$	$A_2 = 44.13\mu M^{-1}$	$\theta = 0.056h^{-1}$
	$\mu_1 = 0.005h^{-1}$	$C_a^0 = 10^{-4}\mu M$		
(13)	$A_r = 10.0\mu Mh^{-1}$	$T_{iv} = 4.1hr.$	$T_{rel} = 1hr.$	
(10)	$\psi_1 = 0.3$	$f_1 = 0.60\mu M$		
(11)	$m_0 = 12$	$\delta = 0.0$	$v_0 = 4.0\mu Mmmh^{-1}$	

References

1. B. Alberts, D. Bray, J. Lewis, M. Raff, K. Roberts & J. D. Watson, (1994) Molecular Biology of the Cell 3rd Ed. Garland Pub. Inc. New York and London.
2. A.R.A. Anderson & M.A.J. Chaplain, (1998), Continuous and Discrete Mathematical Models of Tumour-Induced Angiogenesis. Bull. Math. Biol., **60**, 857-899.
3. J.C. Bowersox & N. Sorgente, (1982), Chemotaxis of Aortic Endothelial Cells in Response to Fibronectin. Cancer Res., **42**, 2547-2551.
4. M.A.J. Chaplain & A.R.A. Anderson, (1999), Modelling the Growth and Forms of Capillary Networks in "On Growth and Form: Spatio-Temporal Pattern Formation in Biology. (Ed. M.A.J. Chaplain, G.D. Singh, J.C. McLachlan), Wiley, 225-249.
5. B. Davis, (1990) Reinforced Random Walks. Probability Theory and Related Fields, **84**, 203-229.
6. D.J. Falcone, K.M. Faisal Khan, T. Lagne & L. Fernandes, (1998), Macrophage Formation of Angiostatin during Inflammation. J. Biological Chemistry, **273**, 31480-31485.
7. J. Folkman, (1985), Tumour Angiogenesis. Adv. Cancer Res., **43**, 175-203.
8. J. Folkman, (1995), Angiogenesis in Cancer, Vascular, Rheumatoid and Other Disease. Nature Medicine, **1**, 21-31.
9. J. Folkman & C. Haudenschild, (1980), Angiogenesis in Vitro. Nature, **288**, 551-556.
10. J. Folkman & M. Klagsbrun, (1987), Angiogenic Factors. Science, **235**, 442-447.
11. D.H. Gorski, H.J. Mauceri, R.M. Salloum, S. Gately, S. Hellmane, M.A. Beckett, V.P. Sukhatme, G.A. Soff, D.W. Kufe & R.R. Weichselbaum, (1998), Potentiation of the Antitumor Effect of Ionizing Radiation by Brief Concomitant Exposures to Angiostates. Cancer Research, **58**, 5686-5689.
12. D. Hanahan & J. Folkman, (1996), Patterns and Emerging Mechanisms of the Angiogenic Switch During Tumorigenesis Cell. **86**, 353-364.
13. M.J. Holmes & B.D. Sleeman, (2000), A Mathematical Model of Tumour Angiogenesis Incorporating Cellular Traction and Viscoelastic Effects. J. Theor. Biol., **202**, 95-112.
14. E. Jendraschak & E. Helene Sage, (1996), Regulation of Angiogenesis by SPARC and Angiostatin: Implications for Tumor Cell Biology. Cancer Biology, **7**, 139-146.
15. H.A. Levine, B.D. Sleeman & M. Nilson-Hamilton (2001a), Mathematical Modeling of the Onset of Capillary Formation Initiating Angiogenesis. J. Math. Biol., **42(3)**, 195-238.
16. H.A. Levine, B.D. Sleeman & M Nilsen-Hamilton, (2000), A Mathematical Model for the Roles of Pericytes and Macrophages in the Onset of Angiogenesis: I, The Role of Protease Inhibitors in Preventing Angiogenesis. Math. Biosciences **168**, 77-115.
17. H.A. Levine & B.D. Sleeman, (1997). A System of Reaction-Diffusion Equations Arising in the Theory of Reinforced Random Walks. S.I.A.M. J. Appl. Math., **57**, 683-730.
18. H.A. Levine, S. Pamuk, B.D. Sleeman & M. Nilsen-Hamilton, (2001b), Mathematical Modeling of Capillary Formation and Development in Tumor Angiogenesis: Penetration into the Stroma, Bull. Math. Biol. **63(5)** 801-863.
19. M.S. O'Reilly, D. Wiederschain, W.G. Stetler-Stevenson, J. Folkman & M.A. Moses, (1999), Regulation of Angiostatin Production by Matrix Metalloproteinase-2 in a Model of Concomitant Resistance. J. Biological Chemistry, **274**, 29568-29571.
20. H.G. Othmer & A. Stevens, (1997), Aggregation, Blow-up and Collapse. The ABCs of Taxis and Reinforced Random Walks. S.I.A.M. J. Appl. Math., **57**, 1044-1081.
21. M.S. Stack, S. Gately, L.M. Bafetti, J. Enghild, J. Soff & G.A. Soff, (1999), Angiostatin in Hibits Endothelial and Melanoma Cellular Invasion by Blocking Matrix-enhanced Plasminogen Activation. Biothem. J., **340**, 77-84.

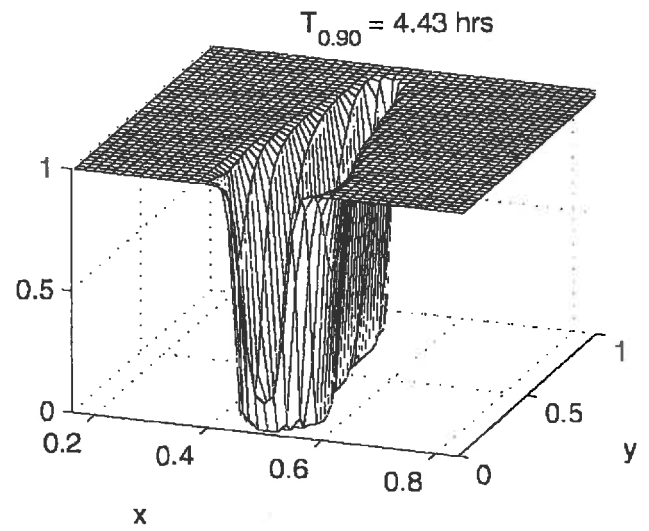
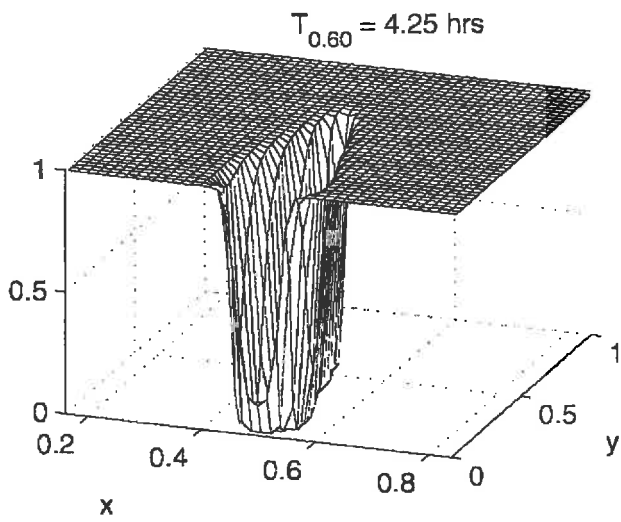
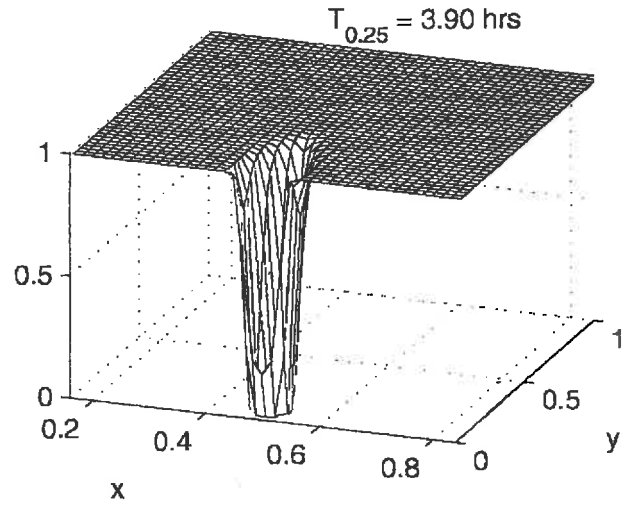
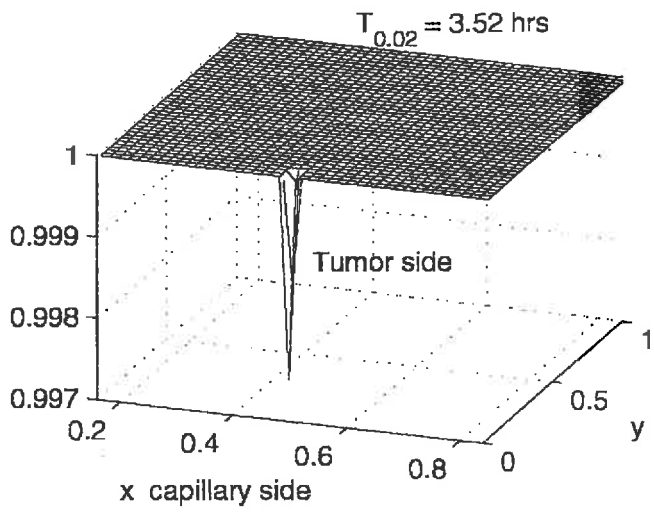
22. B.D. Sleeman, (1996), Solid Tumour Growth: A Case Study in Mathematical Biology in "Nonlinear Mathematics and Its Applications" (Ed. P.J. Aston), C.U.P., 237-256.
23. B.D. Sleeman & I.P. Wallis, (2000), Tumour Induced Angiogenesis as a Reinforced Random Walk: Modelling Capillary Network Formation Without Endothelial Cell Proliferation. J. Comp. Appl. Math., (to appear).
24. C.L. Stokes & D.A. Lauffenburger, (1991), Analysis of the Roles of Microvessel Endothelial Cell Random Motility and Chemotaxis in Angiogenesis. J. Theor. Biol., **152**, 377-403.
25. L. Tranqui & P. Tracqui, (2000), Mechanical Signalling and Angiogenesis. The Integration of Cell-Extracellular Matrix Couplings. C.R. Acad. Sci. Paris, Sciences de la Vie/Life Sciences, **323**, 31-47.



y axis scale: 0.1 = 2.5 microns, x axis scale: 0.1 = 5 microns

Figure 3. Time course for EC propagation in the ECM.

22. B.D. Sleeman, (1996), Solid Tumour Growth: A Case Study in Mathematical Biology in "Nonlinear Mathematics and Its Applications" (Ed. P.J. Aston), C.U.P., 237-256.
23. B.D. Sleeman & I.P. Wallis, (2000), Tumour Induced Angiogenesis as a Reinforced Random Walk: Modelling Capillary Network Formation Without Endothelial Cell Proliferation. J. Comp. Appl. Math., (to appear).
24. C.L. Stokes & D.A. Lauffenburger; (1991), Analysis of the Roles of Microvessel Endothelial Cell Random Motility and Chemotaxis in Angiogenesis. J. Theor. Biol. **152**, 377-403.
25. L. Tranqui & P. Tracqui, (2000), Mechanical Signalling and Angiogenesis. The Integration of Cell-Extracellular Matrix Couplings. C.R. Acad. Sci. Paris, Sciences de la Vie/Life Sciences, **323**, 31-47.



y axis scale: 0.1 = 2.5 microns, x axis scale: 0.1 = 5 microns

Figure 5. Time course for fibronectin propagation in the ECM.

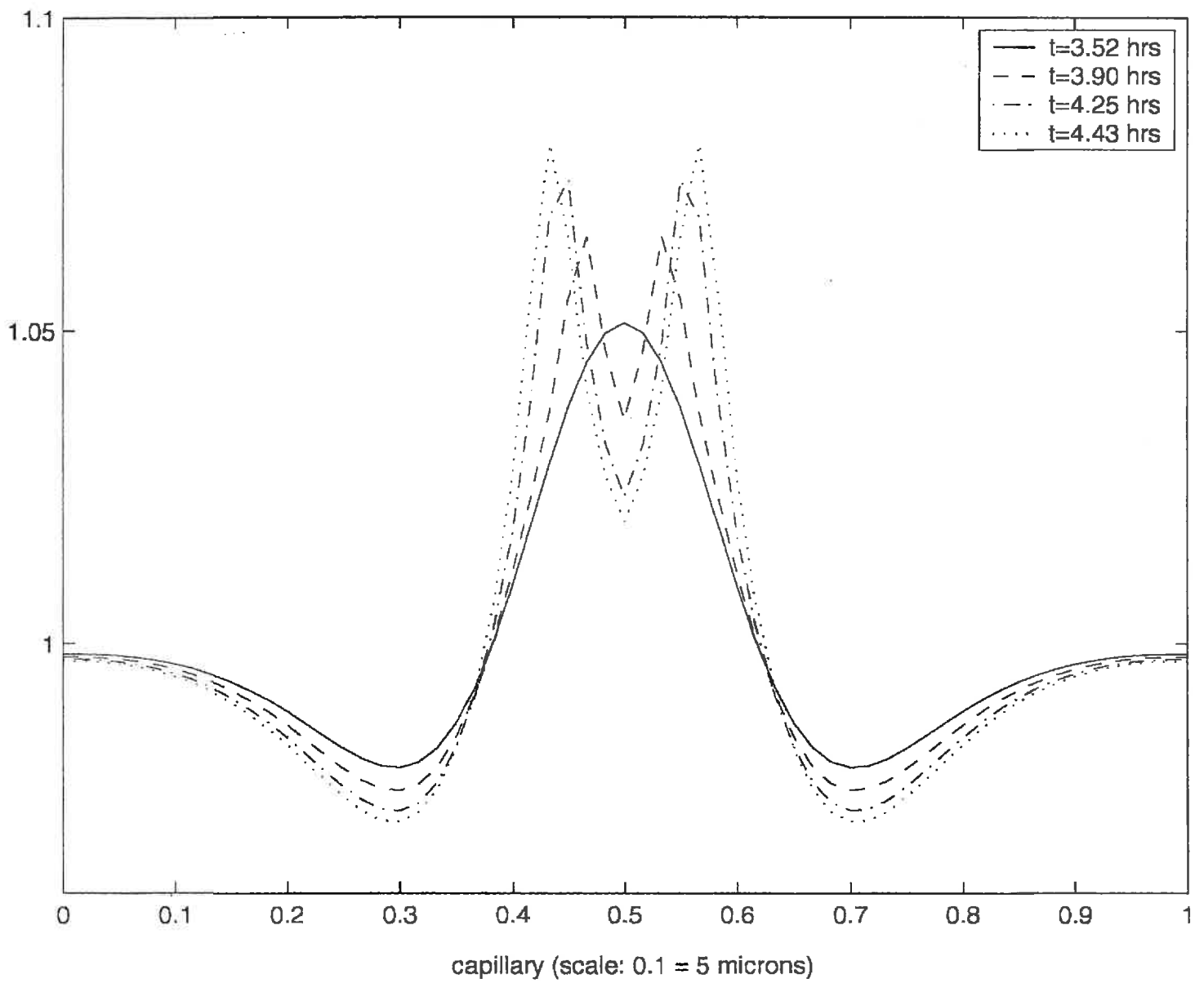
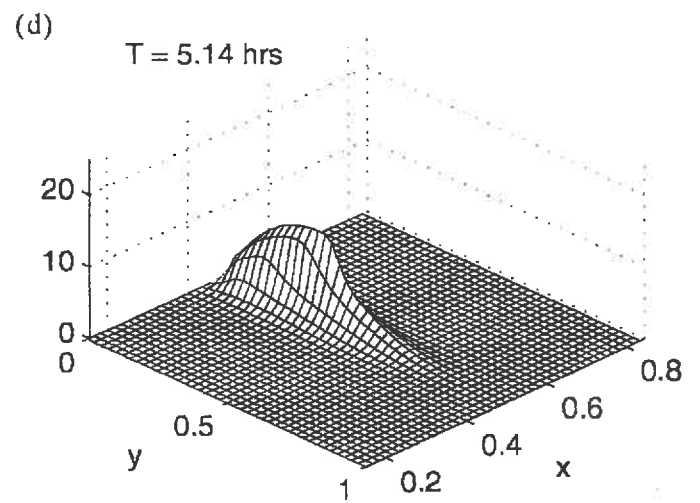
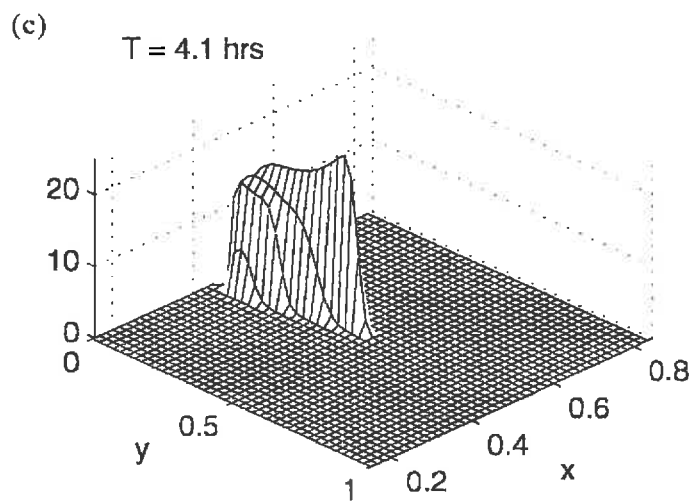
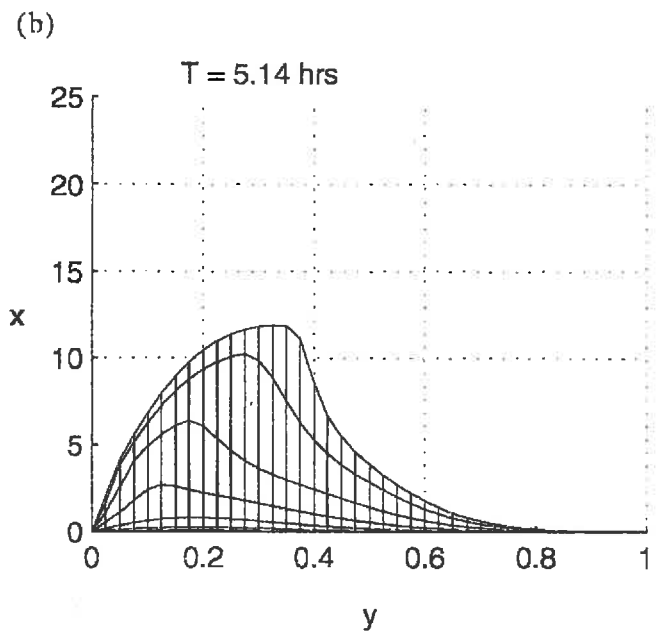
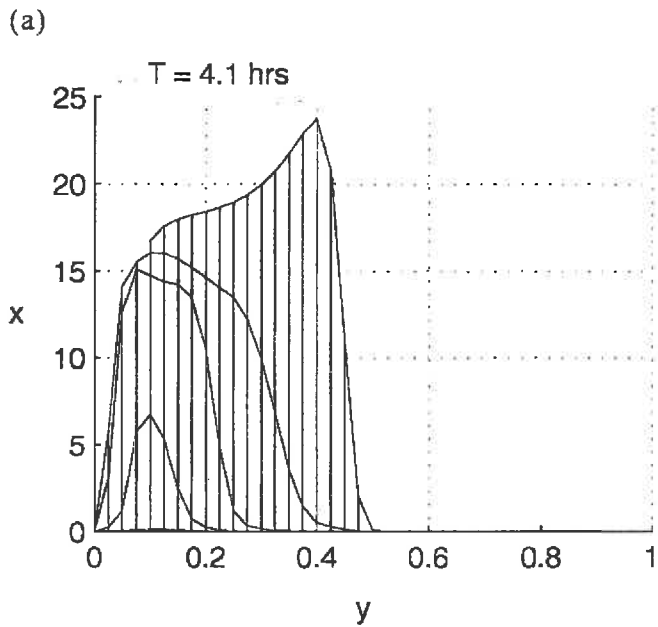


Figure 4. Time course for EC propagation in the capillary.



y axis scale: 0.1 = 2.5 microns, x axis scale: 0.1 = 5 microns
 $y=0$ capillary side, $y=1$ tumor side

Figures 7a-d. Left figures: EC profiles just before inhibitor introduction.
 Right figures: EC profiles after inhibitor introduction.

Top row: EC concentration profile along capillary center.

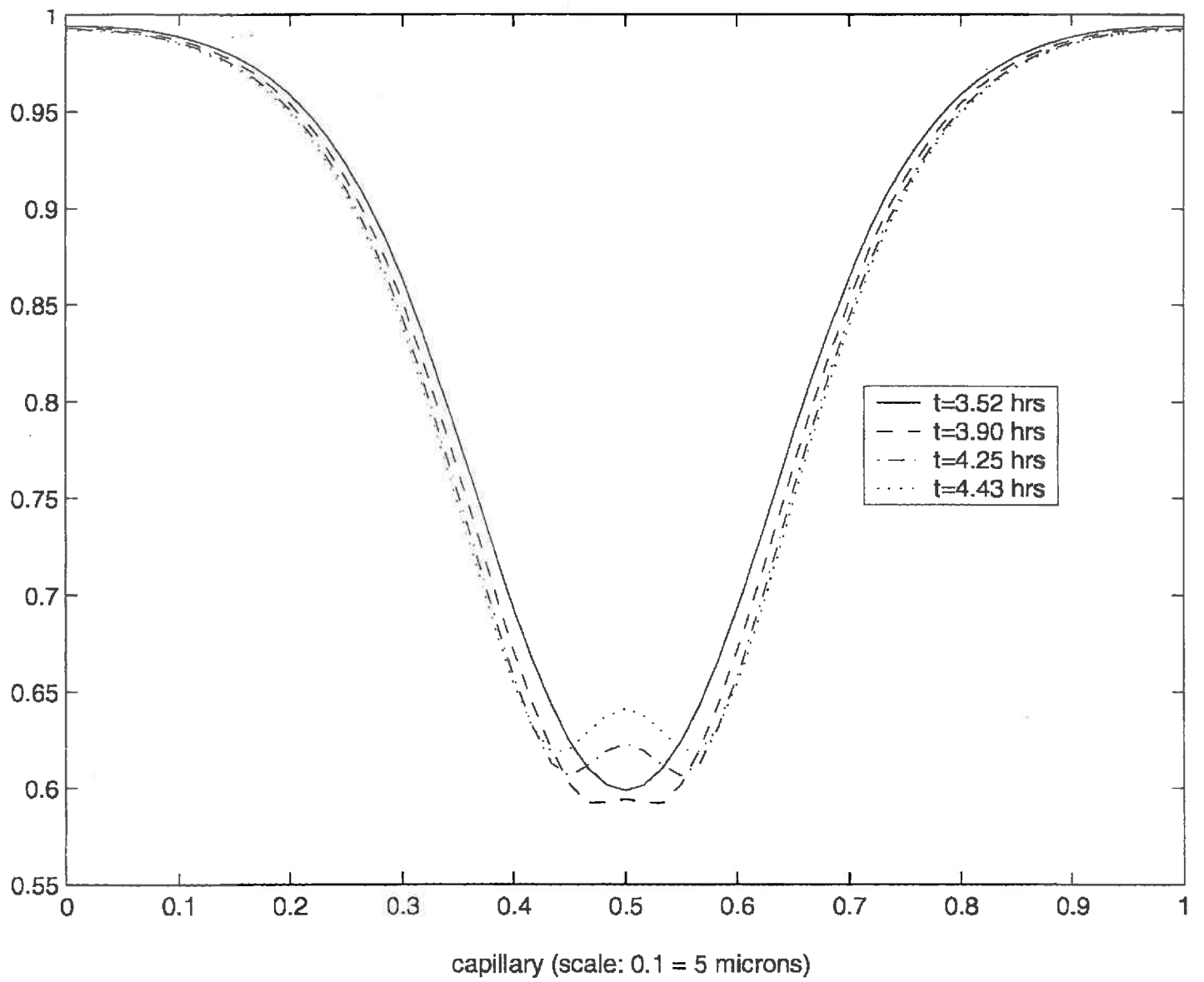


Figure 6. Time course for fibronectin propagation in the capillary.

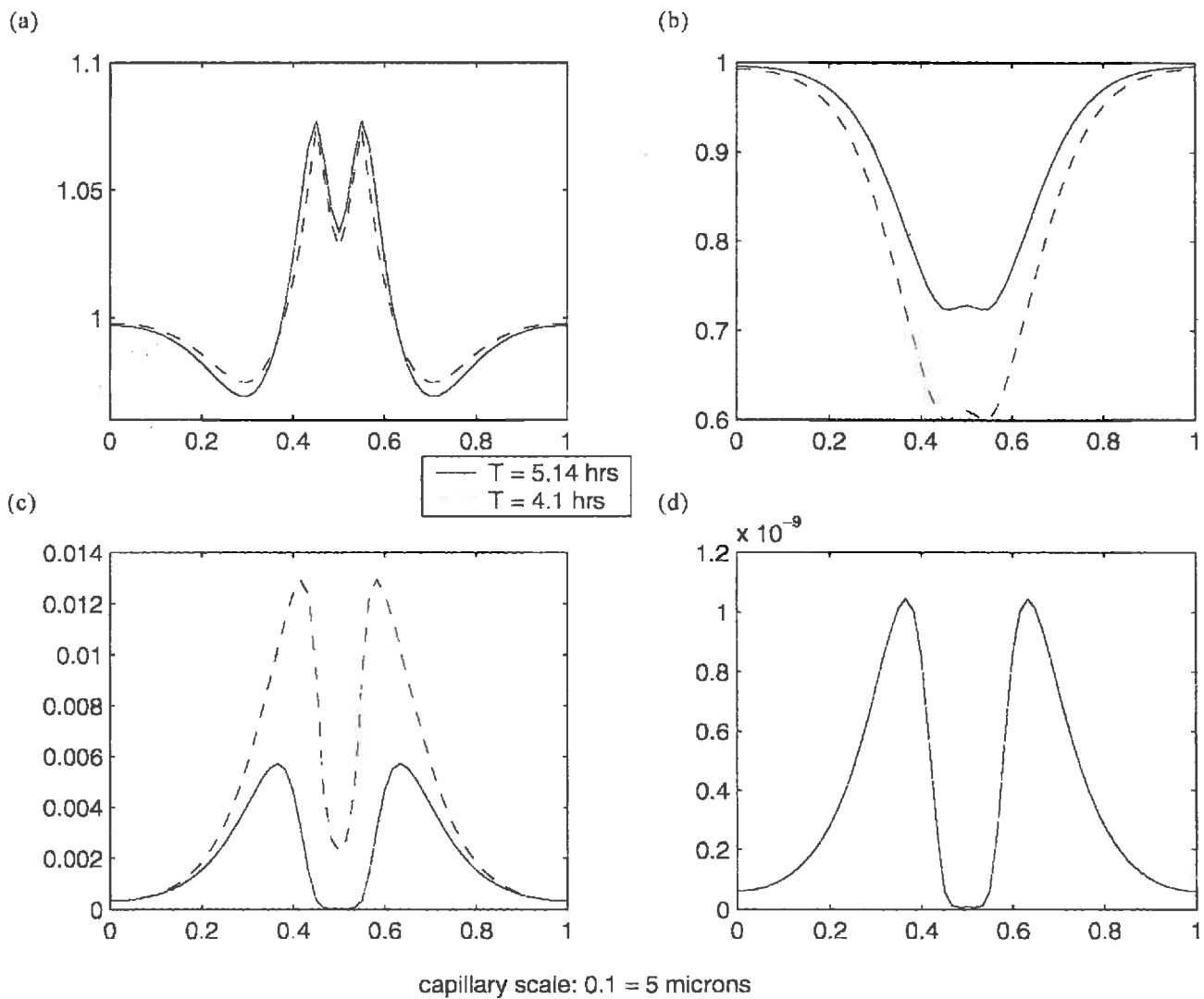


Figure 9a–d. Time courses in the capillary after introduction of inhibitor. 9a: EC time course. 9b: fibronectin time course. 9c: Protease time course. 9d: Active protease time course.

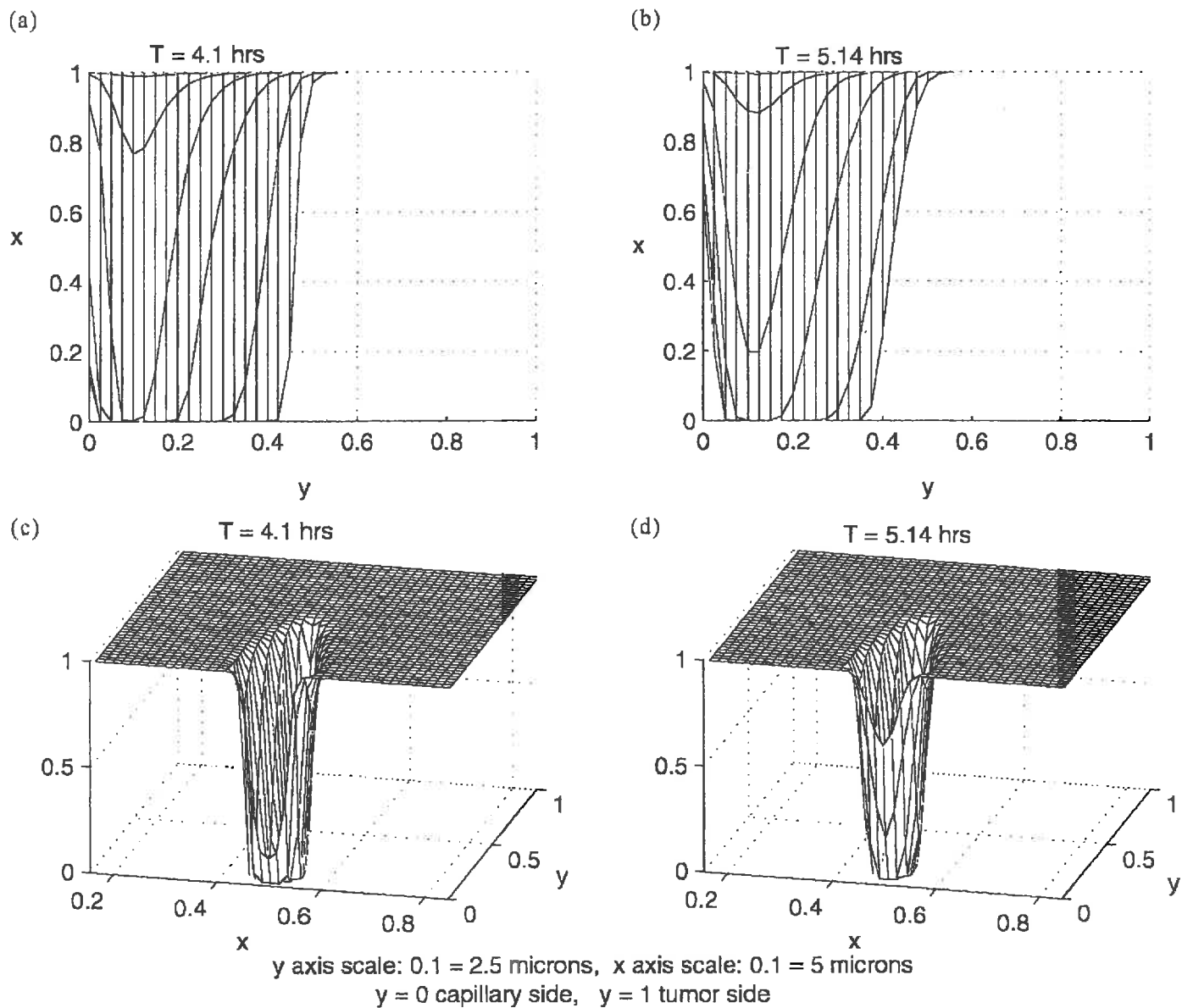
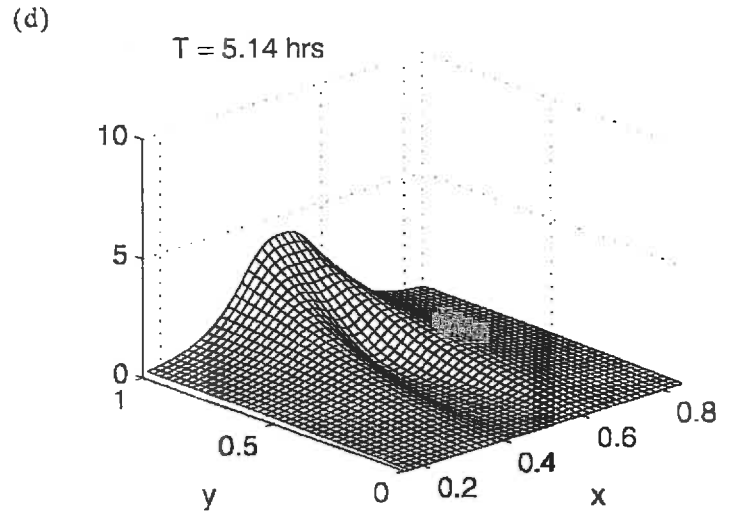
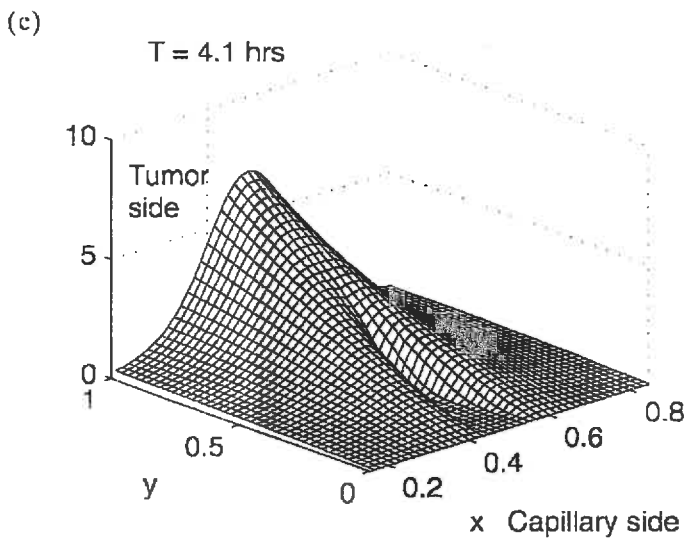
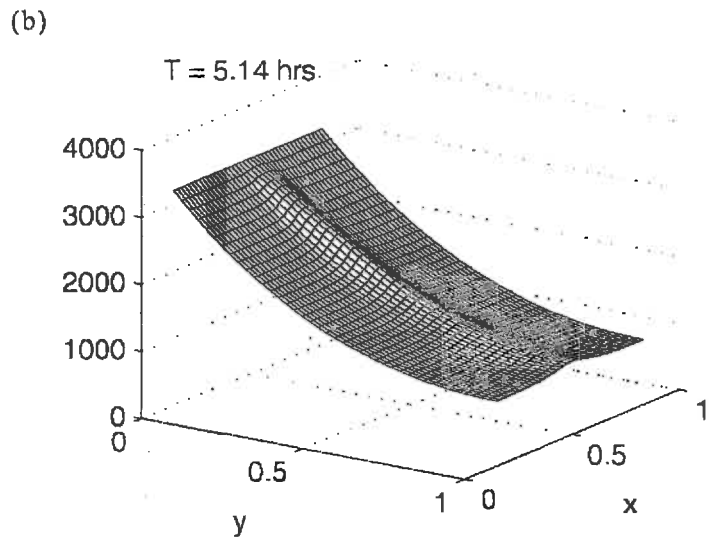
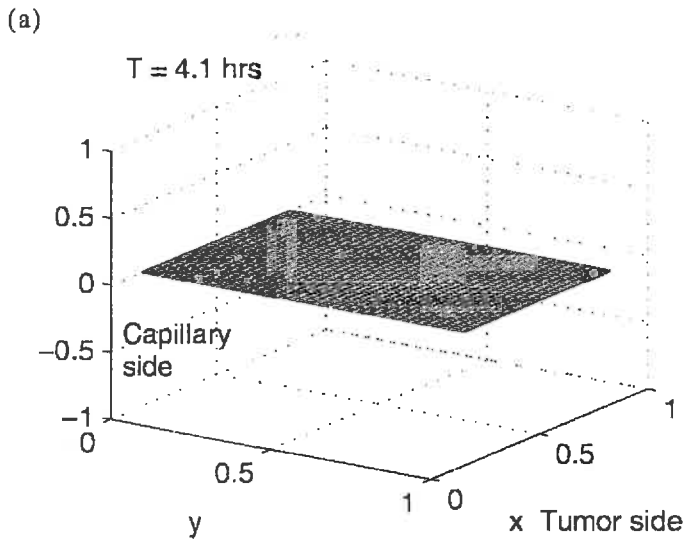


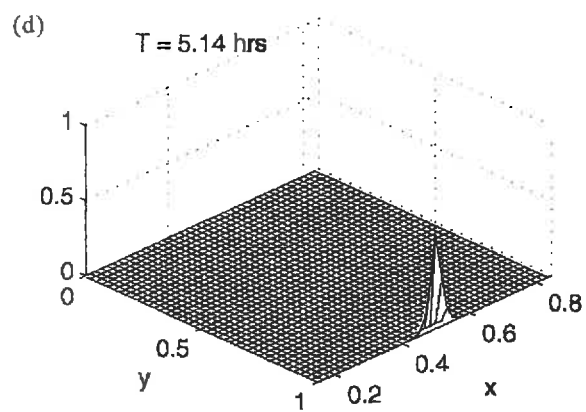
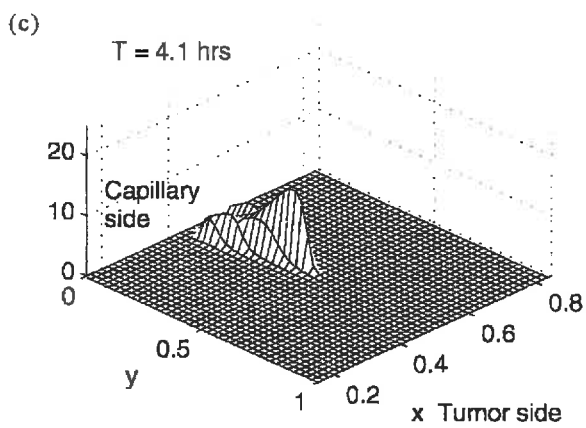
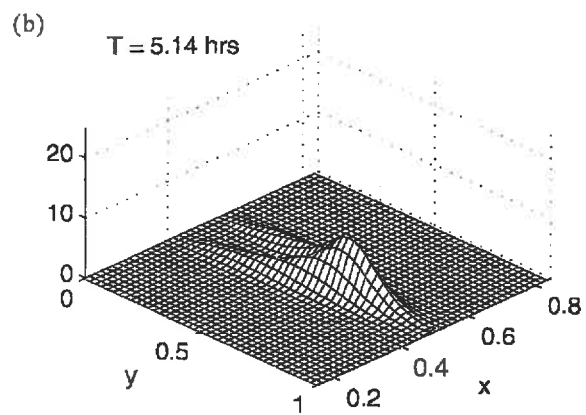
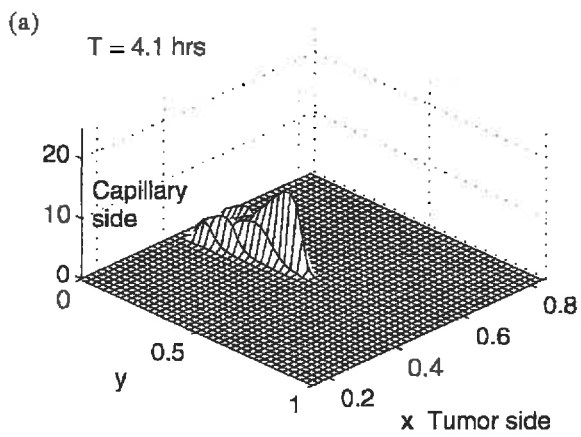
Figure 8 a–d. Time course for fibronectin propagation in the ECM after introduction of inhibitor. Notice that in Figure 8a, the fibronectin density is larger at the capillary opening and near the tip than in Figure 8b. The channel opening is closing here also (8c, d).



y axis scale: 0.1 = 2.5 microns, x axis scale: 0.1 = 5 microns

Figure 10a–d. Figure 10a, b: inhibitor time courses. Figure 10c, d: Growth factor time courses.

Profile



y axis scale: 0.1 = 2.5 microns, x axis scale: 0.1 = 5 microns

Figure 11a, b: Protease time courses after introduction of inhibitor. Figure 11c, d: Active protease time courses.

PROTEASES